

---

# Simulations of Premixed Swirling Flames Using a Hybrid Finite-Volume/Transported PDF Approach

Stefan Lipp<sup>1</sup> and Ulrich Maas<sup>2</sup>

<sup>1</sup> University Karlsruhe, Institute for Technical Thermodynamics,  
lipp@itt.mach.uni-karlsruhe.de

<sup>2</sup> University Karlsruhe, Institute for Technical Thermodynamics  
maas@itt.mach.uni-karlsruhe.de

*Abstract*

The mathematical modeling of swirling flames is a difficult task due to the intense coupling between turbulent transport processes and chemical kinetics in particular for instationary processes like the combustion induced vortex breakdown. In this paper a mathematical model to describe the turbulence-chemistry interaction is presented. The described method consists of two parts. Chemical kinetics are taken into account with reduced chemical reaction mechanisms, which have been developed using the ILDM-Method (“Intrinsic Low-Dimensional Manifold”). The turbulence-chemistry interaction is described by solving the joint probability density function (PDF) of velocity and scalars. Simulations of test cases with simple geometries verify the developed model.

## 1 Introduction

In many industrial applications there is a high demand for reliable predictive models for turbulent swirling flows. While the calculation of non-reacting flows has become a standard task and can be handled using Reynolds averaged Navier-Stokes (RANS) or Large Eddy Simulation (LES) methods the modeling of reacting flows still is a challenging task due to the difficulties that arise from the strong non-linearity of the chemical source term which can not be modeled satisfactorily by using oversimplified closure methods.

PDF methods (probability density function) show a high capability for modeling turbulent reactive flows, because of the advantage of treating convection and finite rate non-linear chemistry exactly [1, 2]. Only the effect of molecular mixing has to be modeled [3]. In the literature different kinds of PDF approaches can be found. Some use stand-alone PDF methods in which all

flow properties are computed by a joint probability density function method [4, 5, 6, 7]. The transport equation for the joint probability density function that can be derived from the Navier-Stokes equations still contains unclosed terms that need to be modeled. These terms are the fluctuating pressure gradient and the terms describing the molecular transport. In contrast the above mentioned chemistry term, the body forces and the mean pressure gradient term already appear in closed form and need no more modeling assumptions. Compared to RANS methods the structure of the equations appearing in the PDF context is remarkably different. The moment closure models (RANS) result in a set of partial differential equations, which can be solved numerically using finite-difference or finite-volume methods [8]. In contrast the transport equation for the PDF is a high-dimensional scalar transport equation. In general it has  $7 + n_S$  dimensions which consist of three dimensions in space, three dimensions in velocity space, the time and the number of species  $n_S$  used for the description of the thermokinetic state. Due to this high dimensionality it is not feasible to solve the equation using finite-difference or finite-volume methods. For that reason Monte Carlo methods have been employed, which are widely used in computational physics to solve problems of high dimensionality, because the numerical effort increases only linearly with the number of dimensions.

Using the Monte Carlo method the PDF is represented by an ensemble of stochastic particles [9]. The transport equation for the PDF is transformed to a system of stochastic ordinary differential equations. This system is constructed in such a way that the particle properties, e.g. velocity, scalars, and turbulent frequency, represent the same PDF as in the turbulent flow.

In order to fulfill consistency of the modeled PDF, the mean velocity field derived from an ensemble of particles needs to satisfy the mass conservation equation [1]. This requires the pressure gradient to be calculated from a Poisson equation. The available Monte Carlo methods cause strong bias determining the convective and diffusive terms in the momentum conservation equations. This leads to stability problems calculating the pressure gradient from the Poisson equation. To avoid these instabilities different methods to calculate the mean pressure gradient were used. One possibility is to couple the particle method with an ordinary finite-volume or finite-difference solver to obtain the mean pressure field from the Navier-Stokes equations. These so called hybrid PDF/CFD methods are widely used by different authors for many types of flames [10, 11, 12, 13, 14, 15].

In the presented paper a hybrid scheme is used. The fields for mean pressure gradient and a turbulence characteristic, e.g. the turbulent time scale, are derived solving the Reynolds averaged conservation equations for momentum, mass and energy for the flow field using a finite-volume method. The effect of turbulent fluctuations is modeled using a  $k$ - $\tau$  model [16]. Chemical kinetics are taken into account by using the ILDM method to get reduced chemical mechanisms [17, 18]. In the presented case the reduced mechanism describes the reaction with three parameters which is on the one hand few enough to

limit the simulation time to an acceptable extent and on the other hand sufficiently high to get a detailed description of the chemical reaction.

The test case for the developed model is a model combustion chamber investigated by several authors [19, 20, 21, 22]. With their data the results of the presented simulations are validated.

## 2 Numerical Model

As mentioned above a hybrid CFD/PDF method is used in this work. In Fig. 1 a complete sketch of the solution procedure can be found. Before explaining the details of the implemented equations and discussing consistency and numerical matters the idea of the solution procedure shall be briefly overviewed. The calculation starts with a CFD step in which the Navier-Stokes equations for the flow field are solved by a finite-volume method. The resulting mean pressure gradient together with the mean velocities and the turbulence characteristics is handed over to the PDF part. Here the joint probability density function of the scalars and the velocity is solved by a particle Monte Carlo method. The reaction progress is taken into account by reading from a lookup table based on a mechanism reduced with the ILDM method. As a result of this step the mean molar mass, the composition vector and the mean temperature field are returned to the CFD part. This internal iteration is performed until convergence is achieved.

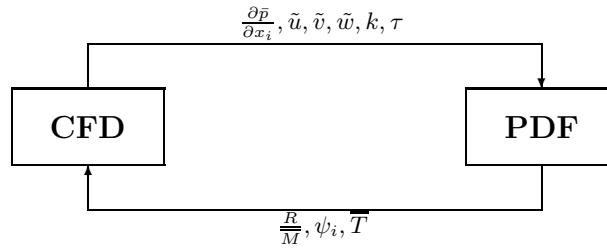


Fig. 1. Scheme of the coupling of CFD and PDF

### 2.1 CFD Model

The CFD code which is used to calculate the mean velocity and pressure field along with the turbulent kinetic energy and the turbulent time scale is called SPARC<sup>3</sup> and was developed by the Department of Fluid Machinery at Karlsruhe University. It solves the Favre-averaged compressible Navier Stokes

<sup>3</sup> Structured Parallel Research Code

equations using a Finite-Volume method on block structured non-uniform meshes. In this work a 2D axi-symmetric solution domain is used. Turbulence closure is provided using a two equation model solving a transport equation for the turbulent kinetic energy and a turbulent time scale [16].

In detail the equations read

$$\frac{\partial \bar{\rho}}{\partial t} + \frac{\partial (\bar{\rho} \tilde{u}_i)}{\partial x_i} = 0 \quad (1)$$

$$\frac{\partial (\bar{\rho} \tilde{u}_i)}{\partial t} + \frac{\partial}{\partial x_j} \left( \bar{\rho} \tilde{u}_i \tilde{u}_j + \overline{\rho u_i'' u_j''} + \bar{\rho} \delta_{ij} - \tau_{ij} \right) = 0 \quad (2)$$

$$\frac{\partial (\bar{\rho} \tilde{e})}{\partial t} + \frac{\partial}{\partial x_j} \left( \bar{\rho} \tilde{u}_j \tilde{e} + \tilde{u}_j \bar{p} + \overline{u_j'' p} + \overline{\rho u_j'' e''} + \bar{q}_j - \overline{u_i \tau_{ij}} \right) = 0 \quad (3)$$

which are the conservation equations for mass, momentum and energy in Favre average manner, respectively. Modeling of the unclosed terms in the energy equation will not be described in detail any further but can be found for example in [8]. The unclosed cross correlation term in the momentum conservation equation is modeled using the Boussinesq approximation

$$\overline{\rho u_i'' u_j''} = \bar{\rho} \mu_T \left( \frac{\partial \tilde{u}_i}{\partial x_j} + \frac{\partial \tilde{u}_j}{\partial x_i} \right) \quad (4)$$

with

$$\mu_T = C_\mu f_\mu k \tau \quad (5)$$

The parameter  $C_\mu$  is an empirical constant with a value of  $C_\mu = 0.09$  and  $f_\mu$  accounts for the influence of walls. The turbulent kinetic energy  $k$  and the turbulent time scale  $\tau$  are calculated from their transport equation which are [16]

$$\bar{\rho} \frac{\partial k}{\partial t} + \bar{\rho} \tilde{u}_j \frac{\partial k}{\partial x_j} = \tau_{ij} \frac{\partial u_i}{\partial x_j} - \bar{\rho} \frac{k}{\tau} + \frac{\partial}{\partial x_i} \left[ \left( \mu + \frac{\mu_T}{\sigma_k} \right) \frac{\partial k}{\partial x_j} \right] \quad (6)$$

$$\begin{aligned} \bar{\rho} \frac{\partial \tau}{\partial t} + \bar{\rho} \tilde{u}_j \frac{\partial \tau}{\partial x_j} &= (1 - C_{\epsilon 1}) \frac{\tau}{k} \tau_{ij} \frac{\partial u_i}{\partial x_j} + (C_{\epsilon 2} - 1) \bar{\rho} + \\ &\frac{\partial}{\partial x_j} \left[ \left( \mu + \frac{\mu_T}{\sigma_{\tau 2}} \right) \frac{\partial k}{\partial x_j} \right] + \frac{2}{k} \left( \mu + \frac{\mu_T}{\sigma_{\tau 1}} \right) \frac{\partial k}{\partial x_k} \frac{\partial \tau}{\partial x_k} - \\ &\frac{2}{\tau} \left( \mu + \frac{\mu_T}{\sigma_{\tau 2}} \right) \frac{\partial \tau}{\partial x_k} \frac{\partial \tau}{\partial x_k} \quad . \end{aligned} \quad (7)$$

Here  $C_{\epsilon 1} = 1.44$  and  $\sigma_{\tau 1} = \sigma_{\tau 2} = 1.36$  are empirical model constants. The parameter  $C_{\epsilon 2}$  is calculated from the turbulent Reynolds number  $\text{Re}_t$ .

$$\text{Re}_t = \frac{k \tau}{\mu} \quad (8)$$

$$C_{\epsilon 2} = 1.82 \left[ 1 - \frac{2}{9} \exp \left( (-\text{Re}_t / 6)^2 \right) \right] \quad (9)$$

## 2.2 Joint PDF Model

In the literature many different joint PDF models can be found, for example models for the joint PDF of velocity and composition [23, 24] or for the joint PDF of velocity, composition and turbulent frequency [25]. A good overview of the different models can be found in [12].

In most joint PDF approaches a turbulent (reactive) flow field is described by a one-time, one-point joint PDF of certain fluid properties. At this level chemical reactions are treated exactly without any modeling assumptions [1]. However, the effect of molecular mixing has to be modeled.

The state of the fluid at a given point in space and time can be fully described by the velocity vector  $\mathbf{V} = (V_1, V_2, V_3)^T$  and the composition vector  $\Psi$  containing the mass fractions of  $n_S - 1$  species and the enthalpy  $h$  ( $\Psi = (\Psi_1, \Psi_2, \dots, \Psi_{n_S-1}, h)^T$ ). The probability density function is

$$f_{\mathbf{U}\phi}(\mathbf{V}, \Psi; \mathbf{x}, t) d\mathbf{V}d\Psi = \text{Prob}(\mathbf{V} \leq \mathbf{U} \leq \mathbf{V} + d\mathbf{V}, \Psi \leq \Phi \leq \Psi + d\Psi) \quad (10)$$

and gives the probability that at one point in space and time one realization of the flow is within the interval

$$\mathbf{V} \leq \mathbf{U} \leq \mathbf{V} + d\mathbf{V} \quad (11)$$

for its velocity vector and

$$\Psi \leq \Phi \leq \Psi + d\Psi \quad (12)$$

for its composition vector.

According to [1] a transport equation for the joint PDF of velocity and composition can be derived. Under the assumption that the effect of pressure fluctuations on the fluid density is negligible the transport equation writes

$$\begin{aligned} & \underbrace{\rho(\Psi) \frac{\partial \tilde{f}}{\partial t}}_I + \underbrace{\rho(\Psi) U_j \frac{\partial \tilde{f}}{\partial x_j}}_{II} + \underbrace{\left[ \left( \rho(\Psi) g_j - \frac{\partial \langle p \rangle}{\partial x_j} \right) \right]}_{III} \frac{\partial \tilde{f}}{\partial U_j} + \underbrace{\frac{\partial}{\partial \Psi_\alpha} \left[ \rho(\Psi) S_\alpha(\Psi) \tilde{f} \right]}_{IV} \\ & = \underbrace{\frac{\partial}{\partial U_j} \left[ \left\langle -\frac{\partial \tau_{ij}}{\partial x_i} + \frac{\partial p'}{\partial x_i} \middle| \mathbf{U}, \Psi \right\rangle \tilde{f} \right]}_V + \underbrace{\frac{\partial}{\partial \Psi_\alpha} \left[ \left\langle -\frac{\partial J_i}{\partial x_i} \middle| \mathbf{U}, \Psi \right\rangle \tilde{f} \right]}_{VI}. \quad (13) \end{aligned}$$

Term I describes the instationary change of the PDF, Term II its change by convection in physical space and Term III takes into account the influence of gravity and the mean pressure gradient on the PDF. Term IV includes the chemical source term which describes the change of the PDF in composition space due to chemical reactions. All terms on the left hand side of the equation appear in closed form, e.g. the chemical source term. In contrast the terms on the right hand side are unclosed and need further modeling. Many closing

assumptions for these two terms exist. In the following only the ones that are used in the present work shall be explained further.

Term V describes the influence of pressure fluctuations and viscous stresses on the PDF. Commonly a Langevin approach [26, 27] is used to close this term. In the presented case the SLM (Simplified Langevin Model) is used [1]. More sophisticated approaches that take into account the effect of non-isotropic turbulence or wall effects exist as well [26, 28]. But in the presented case of a swirling non-premixed free stream flame the closure of the term by the SLM is assumed to be adequate and was chosen because of its simplicity.

Term VI regards the effect of molecular diffusion within the fluid. This diffusion flattens the steep composition gradients which are created by the strong vortices in a turbulent flow. Several models have been proposed to close this term. The simplest model is the interaction by exchange with the mean model (IEM) [29, 30] which models the fact that fluctuations in the composition space relax to the mean. A more detailed model has been proposed by Curl [31] and modified by [32, 33] and is used in its modified form in the presented work. More recently new models based on Euclidian minimum spanning trees have been developed [34, 35] but are not yet implemented in this work.

As mentioned previously it is numerically unfeasible to solve the PDF transport equation with finite-volume or finite-difference methods because of its high dimensionality. Therefore a Monte Carlo method is used to solve the transport equation making use of the fact that the PDF of a fluid flow can be represented as a sum of  $\delta$ -functions.

$$f_{\mathbf{U}, \phi}^*(\mathbf{U}, \Psi; \mathbf{x}, t) = \sum_{i=1}^{N(t)} \delta(\mathbf{v} - \mathbf{u}^i) \delta(\phi - \Psi^i) \delta(\mathbf{x} - \mathbf{x}^i) \quad (14)$$

Instead of the high dimensional PDF transport equation using a particle Monte Carlo method a set of (stochastic) ordinary differential equations are solved for each numerical particle discretizing the PDF. The evolution of the particle position  $\mathbf{X}_i^*$  reads

$$\frac{d\mathbf{X}_i^*}{dt} = \mathbf{U}_i^*(t) \quad (15)$$

in which  $\mathbf{U}_i^*$  is the velocity vector for each particle.

The evolution of the particles in the velocity space can be calculated according to the Simplified Langevin Model [1] by

$$\frac{dU_i^*}{dt} = -\frac{\partial \bar{p}}{\partial x_i} dt - \left( \frac{1}{2} + \frac{3}{4} C_0 \right) [U_i^* - \langle U_i \rangle] \frac{dt}{\tau} + \sqrt{\frac{C_0 k}{\tau}} dW_i \quad . \quad (16)$$

For simplicity the equation is here only written for the  $U$  component of the velocity vector  $\mathbf{U} = (U, V, W)^T$  belonging to the spacial coordinate  $x$  ( $\mathbf{x} = (x, y, z)^T$ ). The equations of the other components  $V, W$  look accordingly. In eqn. 16  $\frac{\partial \bar{p}}{\partial x_i}$  denotes the mean pressure gradient,  $\langle U_i \rangle$  the mean particle velocity,  $t$  the time,  $dW_i$  a differential Wiener increment,  $C_0$  a model constant,

$k$  and  $\tau$  the turbulent kinetic energy and the turbulent time scale, respectively. Finally the evolution of the composition vector can be calculated as

$$\frac{d\Psi}{dt} = S + M \quad (17)$$

in which  $S$  is the chemical source term (appearing in closed form) and  $M$  denotes the effect of molecular mixing. As previously mentioned this term is unclosed and needs further modeling assumptions. For this a modified Curl model is used [32].

### 2.3 Chemical Kinetics

The source term appearing in eqn. 17 is calculated from a lookup table which is created using automatically reduced chemical mechanisms. The deployed technique to create these tables is the ILDM method (“Intrinsic Low-Dimensional Manifold”) by Maas and Pope [17, 18].

The basic idea of this method is the identification and separation of fast and slow time scales. In typical turbulent flames the time scales governing the chemical kinetics range from  $10^{-9}$ s to  $10^2$ s. This is a much larger spectrum than that of the physical processes (e.g. molecular transport) which vary only from  $10^{-1}$ s to  $10^{-5}$ s. Reactions that occur in the very fast chemical time scales are in partial equilibrium and the species are in steady state. These are usually responsible for equilibrium processes. Making use of this fact it is possible to decouple the fast time scales. The main advantage of decoupling the fast time scales is that the chemical system can be described with a much smaller number of variables (degrees of freedom).

In our test case the chemical kinetics are described with only three parameters namely the mixture fraction, the mole fraction of  $\text{CO}_2$  and the mole fraction of  $\text{H}_2\text{O}$  instead of the 34 species (degrees of freedom) appearing in the detailed methane reaction mechanism. Further details of the method and its implementation can be found in [17, 18].

## 3 Results and Discussion

As a test case for the presented model simulations of a premixed, swirling, confined flame are performed. A sketch of the whole test rig is shown in Fig. 2. Details of the test rig and the experimental data can be found in [20, 21, 22].

The test rig consists of a plenum containing a premixed methane-air mixture, a swirl generator, a premixing duct and the combustion chamber itself. In general three different modes exist to stabilize flames. Flames can be stabilized by a small stable burning pilot, by bluff-bodies inserted into the main

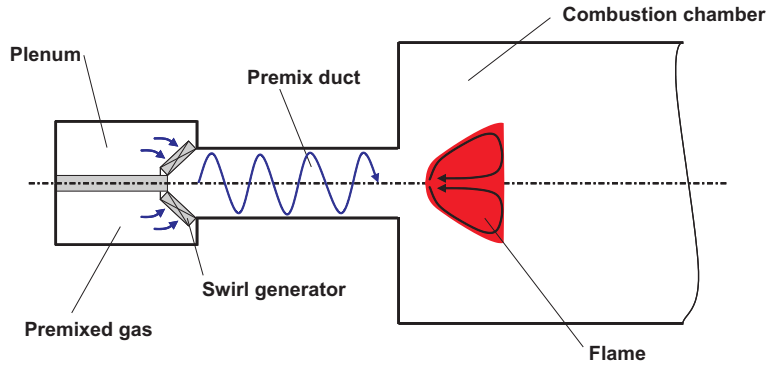


**Fig. 2.** Sketch of the investigated combustion chamber

flow or by aerodynamic arrangements creating a recirculation zone above the burner exit. The last possibility has been increasingly employed for flame stabilization in the gas turbine industry. The recirculation zone (often also abbreviated IRZ<sup>4</sup>) is a region of negative axial velocity close to the symmetry line (see Fig. 2). Heat and radicals are transported upstream towards the flame tip causing a stable operation of the flame. The occurrence and stability of the IRZ depend crucially on the swirl number, the geometry, and the profiles of the axial and tangential velocity.

Simulations were performed using a 2D axi-symmetric grid with approximately 15000 cells. The PDF is discretized with 50 particles per cell. The position of the simulated domain is shown in Fig. 3. Only every fourth grid line is shown for clarity. In this case the mapping of the real geometry (3D) on the 2D axi-symmetric solution domain is possible since the experiments show that all essential features of the flow field exhibit the two dimensional axi-symmetric behaviour [36]. The mapping approach has shown to be valid for the modeling also in [19]. In order to consider the influence of the velocity profiles created by the swirl generator radial profiles of all flow quantities served as inlet boundary conditions. These profiles stem from detailed 3D simulations of the whole test rig using a Reynolds stress turbulence closure and have been taken from the literature [22].

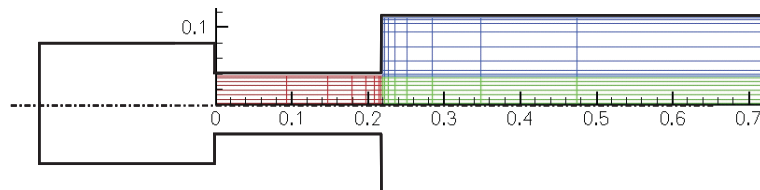


**Fig. 3.** Position of the mesh in the combustion chamber

<sup>4</sup> Internal Recirculation Zone

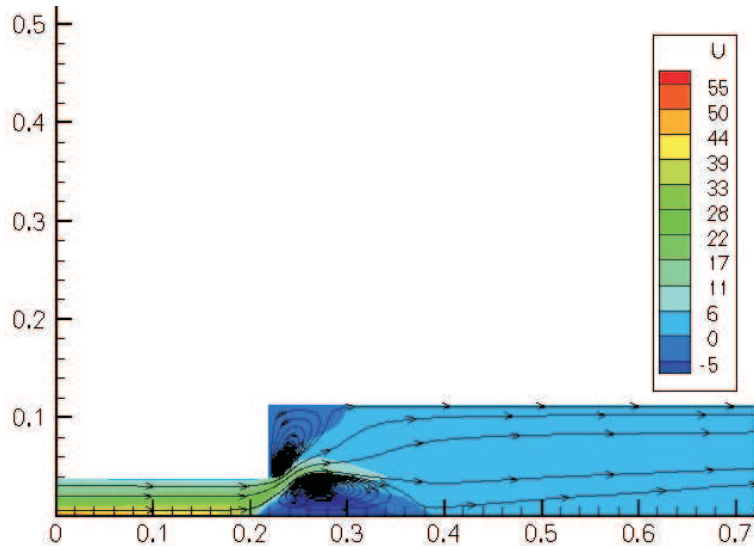
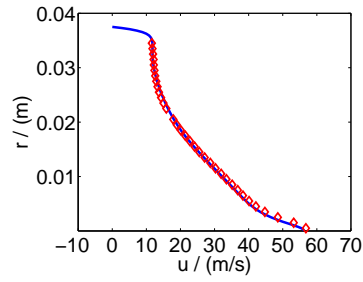


**Fig. 4.** Contourplot of the axial velocity component (with steamtraces)

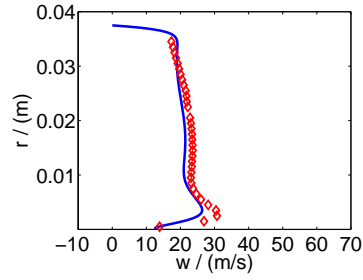
The global operation parameters are an equivalence ratio of  $\phi = 1$ , an inlet mass flow of  $70 \frac{g}{s}$ , a preheated temperature of 373K and a swirl number of  $S = 0.5$ .

First of all simulations of the non-reacting case were done to validate the CFD model and the used boundary conditions which are mapped from the detailed 3D simulations. Fig. 4 shows an example of the achieved results. From the steamtraces one can see two areas with negative axial velocity. One in the upper left corner of the combustion chamber is caused by the step in the geometry and one close to the symmetry line which is caused aerodynamically by the swirl. This area is the internal recirculation zone described above which is in the reactive case used to stabilize the flame. These simulations are validated with experimental results from [20, 21]. The comparison of the experimental data and the results of the simulations for one case are exemplarily shown in Fig. 5 and Fig. 6. In all figures the radial coordinate is plotted over the velocity. Both upper figures show the axial velocity, both lower show the tangential velocity. The lines denote the results of the simulations the scatters denote the results of the measurements. The two axial positions are arbitrarily chosen from the available experimental data. The (relative)  $x$  coordinates refer to the beginning of the premixing duct (Fig. 2). In both cases the profiles of the simulations seem to match reasonably well with the measured data. So the presented model gives a sound description of the flow field of the investigated test case.

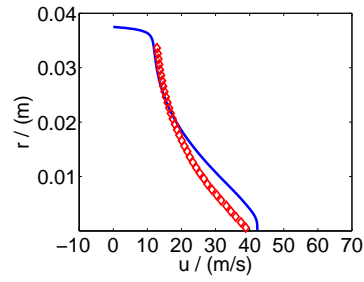
As an example for the reacting case the calculated temperature field of the flame is shown in Fig. 7 which can not be compared to quantitative experiments due to the lack of data. But the qualitative behaviour of the flame is



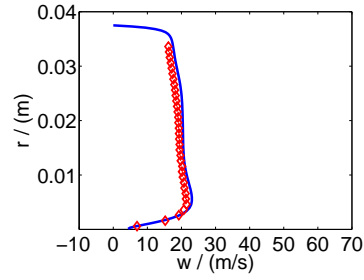
(a) Axial velocity



(b) Tangential velocity

**Fig. 5.**  $x = 29\text{mm}$ 

(a) Axial velocity



(b) Tangential velocity

**Fig. 6.**  $x = 170\text{mm}$ 

predicted correctly. As one can see the tip of the flame is located at the start of the inner recirculation zone. It shows a turbulent flame brush in which the reaction occurs which can be seen in the figure by the rise of temperature. It can not be assessed whether the thickness of the reaction zone is predicted well because no measurements of the temperature field are available.

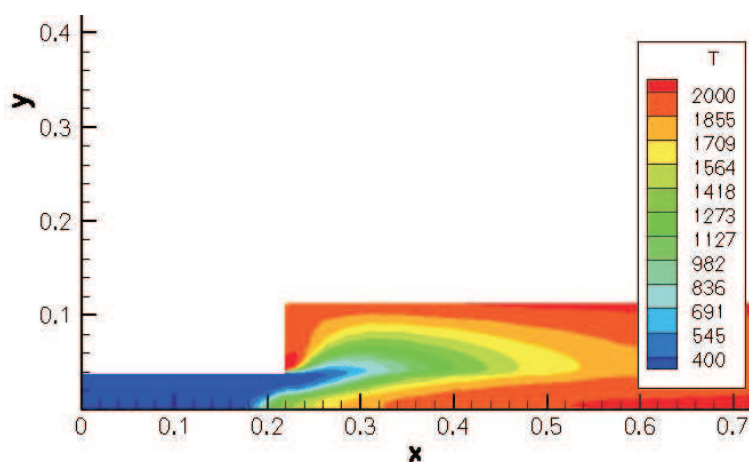


Fig. 7. Temperature field

## 4 Conclusion

Simulations of a premixed swirling methane-air flame are presented. To account for the strong turbulence chemistry interaction occurring in these flames a hybrid finite-volume/transported PDF model is used. This model consists of two parts: a finite volume solver for the mean velocities and the mean pressure gradient and a Monte Carlo solver for the transport equation of the joint PDF of velocity and composition vector. Chemical kinetics are described by automatically reduced mechanisms created with the ILDM method.

The presented results show the validity of the model. The simulated velocity profiles match well with the experimental results. The calculations of the reacting case also show a qualitatively correct behaviour of the flame. A quantitative analysis is subject of future research work.

## References

1. S.B. Pope. Pdf methods for turbulent reactive flows. *Progress in Energy Combustion Science*, 11:119–192, 1985.
2. S.B. Pope. Lagrangian pdf methods for turbulent flows. *Annual Review of Fluid Mechanics*, 26:23–63, 1994.
3. Z. Ren and S.B. Pope. An investigation of the performance of turbulent mixing models. *Combustion and Flame*, 136:208–216, 2004.
4. P.R. Van Slooten and S.B. Pope. Application of pdf modeling to swirling and nonswirling turbulent jets. *Flow Turbulence and Combustion*, 62(4):295–334, 1999.
5. V. Saxena and S.B. Pope. Pdf simulations of turbulent combustion incorporating detailed chemistry. *Combustion and Flame*, 117(1-2):340–350, 1999.

6. S. Repp, A. Sadiki, C. Schneider, A. Hinz, T. Landefeld, and J. Janicka. Prediction of swirling confined diffusion flame with a monte carlo and a presumed-pdf-model. *International Journal of Heat and Mass Transfer*, 45:1271–1285, 2002.
7. K. Liu, S.B. Pope, and D.A. Caughey. Calculations of bluff-body stabilized flames using a joint probability density function model with detailed chemistry. *Combustion and Flame*, 141:89–117, 2005.
8. J.H. Ferziger and M. Peric. *Computational Methods for Fluid Dynamics*. Springer Verlag, 2 edition, 1997.
9. S.B. Pope. A monte carlo method for pdf equations of turbulent reactive flow. *Combustion, Science and Technology*, 25:159–174, 1981.
10. P. Jenny, M. Muradoglu, K. Liu, S.B. Pope, and D.A. Caughey. Pdf simulations of a bluff-body stabilized flow. *Journal of Computational Physics*, 169:1–23, 2000.
11. A.K. Tolpadi, I.Z. Hu, S.M. Correa, and D.L. Burrus. Coupled lagrangian monte carlo pdf-cfd computation of gas turbine combustor flowfields with finite-rate chemistry. *Journal of Engineering for Gas Turbines and Power*, 119:519–526, 1997.
12. M. Muradoglu, P. Jenny, S.B. Pope, and D.A. Caughey. A consistent hybrid finite-volume/particle method for the pdf equations of turbulent reactive flows. *Journal of Computational Physics*, 154:342–370, 1999.
13. M. Muradoglu, S.B. Pope, and D.A. Caughey. The hybrid method for the pdf equations of turbulent reactive flows: Consistency conditions and correction algorithms. *Journal of Computational Physics*, 172:841–878, 2001.
14. G. Li and M.F. Modest. An effective particle tracing scheme on structured/unstructured grids in hybrid finite volume/pdf monte carlo methods. *Journal of Computational Physics*, 173:187–207, 2001.
15. V. Raman, R.O. Fox, and A.D. Harvey. Hybrid finite-volume/transported pdf simulations of a partially premixed methane-air flame. *Combustion and Flame*, 136:327–350, 2004.
16. H.S. Zhang, R.M.C. So, C.G. Speziale, and Y.G. Lai. A near-wall two-equation model for compressible turbulent flows. In *Aerospace Sciences Meeting and Exhibit, 30th, Reno, NV*, page 23. AIAA, 1992.
17. U. Maas and S. B. Pope. Simplifying chemical kinetics: Intrinsic low-dimensional manifolds in composition space. *Combustion and Flame*, 88:239–264, 1992.
18. U. Maas and S.B. Pope. Implementation of simplified chemical kinetics based on intrinsic low-dimensional manifolds. In *Twenty-Fourth Symposium (International) on Combustion*, pages 103–112. The Combustion Institute, 1992.
19. F. Kiesewetter, C. Hirsch, J. Fritz, M. Kröner, and T. Sattelmayer. Two-dimensional flashback simulation in strongly swirling flows. In *Proceedings of ASME Turbo Expo 2003*.
20. M. Kröner. *Einfluss lokaler Löschvorgänge auf den Flammenrückschlag durch verbrennungsinduziertes Wirbelaufplatzen*. PhD thesis, Technische Universität München, Fakultät für Maschinenwesen, 2003.
21. J. Fritz. *Flammenrückschlag durch verbrennungsinduziertes Wirbelaufplatzen*. PhD thesis, Technische Universität München, Fakultät für Maschinenwesen, 2003.
22. F. Kiesewetter. *Modellierung des verbrennungsinduzierten Wirbelaufplatzens in Vormischbrennern*. PhD thesis, Technische Universität München, Fakultät für Maschinenwesen, 2005.

23. D.C. Haworth and S.H. El Tahry. Probability density function approach for multidimensional turbulent flow calculations with application to in-cylinder flows in reciprocating engines. *AIAA Journal*, 29:208, 1991.
24. S.M. Correa and S.B. Pope. Comparison of a monte carlo pdf finite-volume mean flow model with bluff-body raman data. In *Twenty-Fourth Symposium (International) on Combustion*, page 279. The Combustion Institute, 1992.
25. W.C. Welton and S.B. Pope. Pdf model calculations of compressible turbulent flows using smoothed particle hydrodynamics. *Journal of Computational Physics*, 134:150, 1997.
26. D.C. Haworth and S.B. Pope. A generalized langevin model for turbulent flows. *Physics of Fluids*, 29:387–405, 1986.
27. H.A. Wouters, T.W. Peeters, and D. Roekaerts. On the existence of a generalized langevin model representation for second-moment closures. *Physics of Fluids*, 8, 1996.
28. T.D. Dreeben and S.B. Pope. Pdf/monte carlo simulation of near-wall turbulent flows. *Journal of Fluid Mechanics*, 357:141–166, 1997.
29. C. Dopazo. Relaxation of initial probability density functions in the turbulent convection of scalar fields. *Physics of Fluids*, 22:20–30, 1979.
30. P.A. Libby and F.A. Williams. *Turbulent Reacting Flows*. Academic Press, 1994.
31. R.L. Curl. Dispersed phase mixing: 1. theory and effects in simple reactors. *A.I.Ch.E. Journal*, 9:175,181, 1963.
32. J. Janicka, W. Kolbe, and W. Kollmann. Closure of the transport equation of the probability density function of turbulent scalar fields. *Journal of Non-Equilibrium Thermodynamics*, 4:47–66, 1979.
33. S.B. Pope. An improved turbulent mixing model. *Combustion, Science and Technology*, 28:131–135, 1982.
34. S. Subramaniam and S.B. Pope. A mixing model for turbulent reactive flows based on euclidean minimum spanning trees. *Combustion and Flame*, 115(4):487–514, 1999.
35. S. Subramaniam and S.B. Pope. Comparison of mixing model performance for nonpremixed turbulent reactive flow. *Combustion and Flame*, 117(4):732–754, 1999.
36. J. Fritz, M. Kroëner, and T. Sattelmayer. Flashback in a swirl burner with cylindrical premixing zone. In *Proceedings of ASME Turbo Expo 2001*.